Send Orders for Reprints to reprints@benthamscience.ae

The Open Fuels & Energy Science Journal, 2015, *8*, 63-67

Open Access

Wellbore Flow Analysis of a Gas-Kick Well During Shut-In

Sun Shihui*, Yan Tie, Bi Xueliang, Chen Xun and Zhang Nan

Institute of Petroleum Engineering, Northeast Petroleum University, Daqing 163318, China

Abstract: Due to the effects of wellbore storage, shut-in period allows additional inflow of gas bubbles into the annulus. Wellbore and casing pressures rise during shut-in of a gas kick as a consequence of gas upward migration and gas compressibility, which will threaten the safety of well control. Therefore, the variation law of surface and wellbore pressures for a gas kick well during shut-in should be investigated. Based on wellbore storage effect, a new model to the wellbore and casing pressure build-up during shut-in for a gas kick well is developed in this paper. Simulation results show that at different gas kick volumes, the rate of bottom-hole pressure rise increases as the permeability decreases. And surface casing pressure stabilizes quickly for low permeable formations. However, at equal initial annular gaseous volume, the rates of rise of the bottom-hole and surface casing pressures for low permeable formations are slower than for high permeability formations.

Keywords: Bottom hole pressure, casing pressure, gas kick, well shut-in, wellbore storage effects.

1. INTRODUCTION

Due to the effect of wellbore storage, shut-in period allows additional inflow of gas bubbles into the annulus. Gas bubbles migrate upward, wellbore and casing pressures rise with increase in shut-in time that can lead to weak formation leakage, wellhead equipment breakdown and other drilling accidents [1-3]. All of the currently existing models for pressure analysis are based on gas upward migration approach [4, 5]. However, gas compressibility also play a significant role in the pressure build-up. Because of the compressibility of gas phase in annular fluid system, the initial total annular volume occupied by the gas is reduced. Therefore, the pressurization by the formation would introduce an equivalent volume of gas bubble into the annulus to retain the initial annular volume of the gaseous phase at all times. By this action, the annular gas phase volume is kept constant with increased mass of the gaseous phase. This causes the gas density to correspondingly increase with time. Surface casing and the bottom hole or wellbore pressures stabilized until the bottom-hole pressure equalizes the gas reservoir pressure. Therefore, the variation laws of surface and wellbore pressures which are caused by upward gas migration and gas compressibility at well shut-in should be investigated. The primary objective of this paper is to implement the wellbore storage concept to analyzing pressure rise in the wellbore and at the surface when the well is shut-in.

2. ANNULAR PRESSURE MODEL OF A GAS-KICK WELL DURING SHUT-IN

For the wellbore pressure modeling, the following hypotheses are considered in this study.

1. The continuous phase, drilling mud is static, while the dispersed phase, gas is allowed to migrate upward with no further expansion after well complete closure.
2. Drilling mud is assumed incompressible, while the gas phase is considered highly compressible.
3. The effect of the weight of cuttings on the bottom hole pressure is neglected.
4. The time taken to shut in the well is assumed to be known.

Since the annulus comprises mostly of incompressible drilling mud and some highly compressible gaseous phase, the annular fluid system is considered to be slightly compressible. That is, not as compressible as when the entire annulus is filled with gas. For slightly compressible fluid system, the standard compressibility expression under isothermal condition can be expressed as follow [6].

$$C_{\rm g} = \frac{1}{\rho_{\rm g}} \frac{{\rm d}\rho_{\rm g}}{{\rm d}P_{\rm bh}} \tag{1}$$

By applying Chain Rule, Eq. (1) can be expressed as follow [7].

$$C_{\rm g} = \frac{1}{\rho_{\rm g}} \frac{{\rm d}\rho_{\rm g}}{{\rm d}t} \frac{{\rm d}t}{{\rm d}P_{\rm bh}} \tag{2}$$

Re-arranging Eq. (2), we have:

$$\frac{{\rm d}P_{\rm bh}}{{\rm d}t} = \frac{1}{\rho_{\rm g} C_{\rm g}} \frac{{\rm d}\rho_{\rm g}}{{\rm d}t} \tag{3}$$

Gas density is expressed as follows:

$$\rho_{\rm g} = \frac{m_{\rm g}}{q_{\rm g}} \tag{4}$$

*Address correspondence to this author at the College of Petroleum Engineering, Northeast Petroleum University, Daqing 163318, Heilongjiang, China; Tel: 0459-6500886; E-mail: sshsmile@163.com

1876-973X/15 2015 Bentham Open

where, C_g is gas compressibility, Pa^{-1}; ρ_g is gas density, kg/m^3; P_{bh} is bottomhole pressure, Pa; m_g is mass of gas bubble, kg; and q_g is the portion of the annular volume occupied by the gas, m^3/min.

Differentiating Eq. (4) with respect to time, t, yields:

$$\frac{d\rho_g}{dt} = \frac{q_g \frac{dm_g}{dt} - m_g \frac{dq_g}{dt}}{q_g^2} \tag{5}$$

At any instantaneous time, t, any pressure imposed on the annular gas compresses a constant gas mass that causes additional gas inflow from the reservoir. Such compression results in increased gas mass of the entire annular gaseous phase at instantaneous time $t+\Delta t$ for the constant annular gas volume. However, the mass of each already existing gas bubble, before the additional inflow, is assumed to remain the same. Therefore, the increase in the entire annular gaseous mass is as a result of the additional gas inflow by the wellbore storage effect. It should be noted that the consequential change in density for each of the gas bubble is due to the change in its volume only. Thus, at any instant, the reservoir pressurizes a constant annular gaseous mass for additional inflow. At that instant of reservoir pressurization,

$$\frac{dm_g}{dt} \approx 0 \tag{6}$$

Also, since the successive additional gas bubbles are as a result of reduction in the entire annular gaseous volume, substituting Eq. (6) into Eq. (5) yields an expression in terms of the gas density and volume:

$$\frac{d\rho_g}{dt} = \frac{\rho_g}{q_g}\frac{dq_g}{dt} \tag{7}$$

When Eq. (7) is substituted into Eq. (3), we have:

$$\frac{dP_{bh}}{dt} = \frac{1}{q_g C_g}\frac{dq_g}{dt} \tag{8}$$

Gas inflow rate is expressed as: $q_g = \frac{Kh(P_p^2 - P_{bh}^2)B_g}{P_D (T\mu_g Z_g)_{res}}$ [8], so re-arranging Eq. (8) yields:

$$\frac{dP_{bh}}{P_p^2 - P_{bh}^2} = \frac{1}{C_g q_g}\frac{KhB_g}{T_{bh}\mu_g Z_g}\frac{dt}{P_D} \tag{9}$$

Two constant parameters could be defined as follows:

$$I_c = \frac{K}{\phi C_g \mu_g r_w^2}$$

and,

$$J_c = \ln I_c + 0.81$$

where, K is formation permeability, m^2; h is formation interval or height drilled, m; B_g is gas formation volume factor, m^3/m^3; μ_g is gas viscosity, Pa·s; Z_g is gas compressibility factor, 1; P_D is dimensionless wellbore pressure parameter, 1; P_p is formation pore pressure, Pa; T is wellbore temperature, K; T_{bh} is bottom hole temperature, K; ϕ is formation porosity, 1; r_w is wellbore radius, m.

Therefore, dimensionless pressure term simplifies to:

$$P_D = \frac{1}{2}\left(J_c + \ln t\right) \tag{10}$$

Substituting Eq. (10) into Eq. (9) and integrating results, we have:

$$\int \frac{dP_{bh}}{P_p^2 - P_{bh}^2} = \frac{1}{C_g q_g}\frac{KhB_g}{T_{bh}\mu_g Z_g}\int \frac{2dt}{J_c + \ln t} \tag{11}$$

where the Left-Hand-Side of Eq. (11) is integrated as:

$$\int \frac{dP_{bh}}{P_p^2 - P_{bh}^2} = \frac{1}{P_p}\tanh^{-1}\frac{P_{bh}}{P_p} \tag{12}$$

Let,

$$u = J_c + \ln t \tag{13}$$

Differentiating Eq. (13) with respect to time, t, we have:

$$du = \frac{1}{t}dt \tag{14}$$

Then,

$$dt = t\,du \tag{15}$$

From Eq. (13),

$$\ln t = u - J_c$$

Then,

$$t = e^{(u - J_c)} \tag{16}$$

Therefore, substituting Eq. (15) and (16) into the Right-Hand-Side of Eq. (11), we have:

$$\int \frac{dt}{J_c + \ln t} = \int \frac{e^{(u-J_c)}}{u}du = \frac{1}{e^{J_c}}\int \frac{e^u}{u}du \tag{17}$$

The Right-Hand-Side integrand is evaluated as:

$$\int \frac{e^u}{u}du = \ln u + \frac{u}{1\cdot 1!} + \frac{u^2}{2\cdot 2!} + \frac{u^3}{3\cdot 3!} + \frac{u^4}{4\cdot 4!} + \frac{u^5}{5\cdot 5!} + \cdots \tag{18}$$

So, substitution of Eq. (18) into Eq. (17) yields:

$$\int \frac{dt}{J_c + \ln t} = \frac{1}{e^{J_c}}\left[\begin{array}{l} \ln\left(J_c + \ln t\right) + \frac{\left(J_c + \ln t\right)}{1\cdot 1!} + \frac{\left(J_c + \ln t\right)^2}{2\cdot 2!} \\ + \frac{\left(J_c + \ln t\right)^3}{3\cdot 3!} + \frac{\left(J_c + \ln t\right)^4}{4\cdot 4!} + \frac{\left(J_c + \ln t\right)^5}{5\cdot 5!} + \cdots \end{array}\right] \tag{19}$$

If a parameter is defined as:

$$\delta = \ln\left(J_c + \ln t\right) + \frac{\left(J_c + \ln t\right)}{1\cdot 1!} + \frac{\left(J_c + \ln t\right)^2}{2\cdot 2!} + \frac{\left(J_c + \ln t\right)^3}{3\cdot 3!} + \frac{\left(J_c + \ln t\right)^4}{4\cdot 4!} + \frac{\left(J_c + \ln t\right)^5}{5\cdot 5!} + \cdots$$

Then, substituting Eqs. (12) and (19) into the solution of the model Eq. (11), completely solves for the model.

Therefore, we have the complete solution expressed as follows:

$$\frac{1}{P_{\mathrm{p}}}\tanh^{-1}\frac{P_{\mathrm{bh}}}{P_{\mathrm{p}}}=\frac{2}{e^{J_{\mathrm{c}}}}\frac{1}{C_{\mathrm{g}}q_{\mathrm{g}}}\frac{KhB_{\mathrm{g}}}{T_{\mathrm{bh}}\mu_{\mathrm{g}}Z_{\mathrm{g}}}+C_1 \tag{20}$$

For simplicity sake, another arbitrary parameter can be defined as:

$$\Pi=\frac{2}{e^{J_{\mathrm{c}}}}\frac{1}{C_{\mathrm{g}}q_{\mathrm{g}}}\frac{KhB_{\mathrm{g}}}{T_{\mathrm{bh}}\mu_{\mathrm{g}}Z_{\mathrm{g}}}$$

Therefore, Eq. (20) is re-written as:

$$P_{\mathrm{bh}}=P_{\mathrm{p}}\tanh\left[P_{\mathrm{p}}\left(\Pi\delta+C_1\right)\right] \tag{21}$$

When $P=P_{\mathrm{hy}}$ is substituted into Eq. (21), the constant of integration is solved for as:

$$C_1=\frac{1}{P_{\mathrm{p}}}\tanh^{-1}\left(\frac{P_{\mathrm{hy}}}{P_{\mathrm{p}}}\right)-\Pi\delta\Big|_{t=t_{\mathrm{shut}}} \tag{22}$$

According to Eq. (1), gas density in bottom hole is determined as:

$$\rho_{\mathrm{g}}=e^{\left(P_{\mathrm{bh}}-C_2\right)C_{\mathrm{g}}} \tag{23}$$

where C_2 is another constant of integration, and it is expressed in terms of the reservoir conditions as:

$$C_2=P_{\mathrm{p}}-\frac{1}{C_{\mathrm{g,res}}}\ln\rho_{\mathrm{g,res}} \tag{24}$$

Annular gas volumetric fraction is represented as follow [9].

$$\lambda_{\mathrm{g}}=\frac{q_{\mathrm{g}}}{q_{\mathrm{g}}+q_{\mathrm{l}}} \tag{25}$$

Implementing a volumetric averaging technique, the average density of the annular fluid system is estimated as follow [10].

$$\rho_{\mathrm{f}}=\frac{\rho_{\mathrm{g}}q_{\mathrm{g}}+\rho_{\mathrm{l}}q_{\mathrm{l}}}{q_{\mathrm{g}}+q_{\mathrm{l}}}=\rho_{\mathrm{g}}\lambda_{\mathrm{g}}+\rho_{\mathrm{l}}\left(1-\lambda_{\mathrm{g}}\right) \tag{26}$$

Therefore, the hydrostatic pressure of the annular fluid system can be estimated from:

$$P_{\mathrm{hy}}=\rho_{\mathrm{f}}gH \tag{27}$$

where, q_{l} is drilling fluid flow rate, m^3/min; ρ_{l} is liquid density, kg/m^3; g is gravity acceleration, m/s^2.

The annular fluid hydrostatic pressure in Eq. (27) is computed for every wellbore buildup pressure value to obtain the corresponding surface casing pressure rise.

$$P_{\mathrm{c}}=P_{\mathrm{bh}}-P_{\mathrm{hy}} \tag{28}$$

Eq. (21) and (28) can be used to predict bottom-hole pressure and surface casing pressure when gas kick volume is q_{g}.

3. DYNAMIC SIMULATION OF A GAS-KICK WELL DURING SHUT-IN

3.1. Simulation of Gas Migration at Different Gas Kick Volumes

At the same rate of penetration and for the same interval drilled into the reservoir of different permeability values of 50-md, 300-md and 400-md, Figs. (**1**-**3**) show the trends of bottom hole pressure, inflow gas volume and surface casing pressure with shut-in time for a wellbore shut-in during a gas kick.

As seen in Fig. (**1**), gas bubbles migrate upward and expand in wellbore, due to the limitation of annular volume, bottom hole pressure build-up as shut-in time increases. And when bottom hole pressure increases to balance with formation pressure, wellbore pressure will be stable.

Also, the rate of bottom-hole pressure rise increases as the permeability decreases. This is because at the time of noticing a gas-kick on surface equipment, drilling a low permeable reservoir would have caused a smaller volume of gas inflow into the annulus than drilling the same interval into a higher permeable reservoir. The smaller the gas fraction is, the higher the bottom hole pressure is. In the meantime, for the same reservoir pressure imposed on different annular gas volumes, it takes a shorter time to compress a smaller gas volume to its maximum density than compressing a larger gas volume to the same maximum density. Therefore, low permeable formations would build-up its wellbore pressure faster than highly permeable formations. Surface casing pressure observed in the field should be expected to stabilize quickly for low permeable formations.

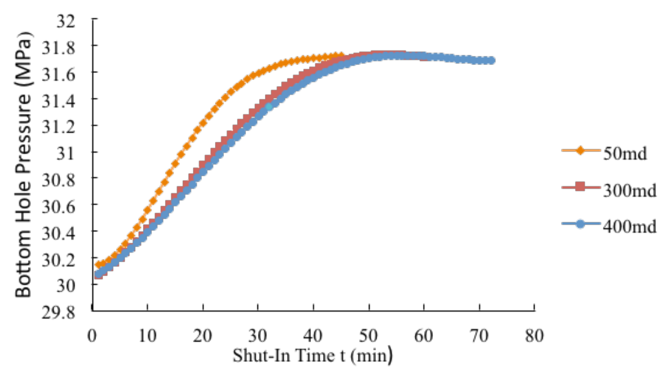

Fig. (1). Bottom hole pressure for different permeability values during shut-in.

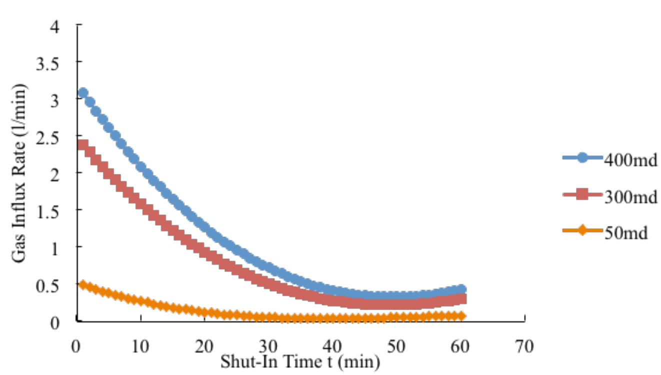

Fig. (2). Inflow gas volume for different permeability values during shut-in.

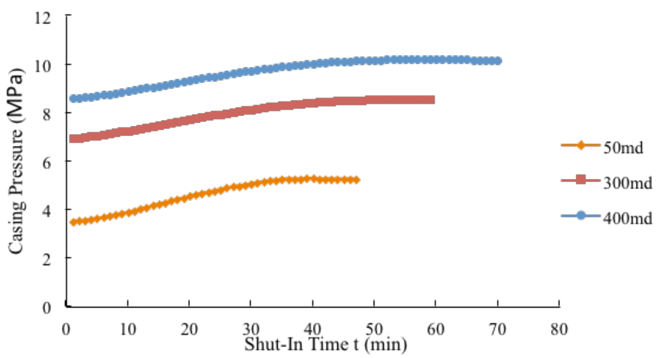

Fig. (3). Surface casing pressure for different permeability values during shut-in.

Since the gas bubbles in annular fluid system are capable of further compression, shut-in period allows additional inflow of gas bubbles into the annulus with the effect of wellbore storage. Under the same reservoir pressure for all the permeability cases, Fig. (**2**) shows that as shut-in time increases, the rate of inflow decline. This is because wellbore pressure buildup during shut-in of a gas kick, pressure difference between the wellbore and formation decreases, and the subsequent inflow rate decline. And as shown in Fig. (**2**), lower gas flow rate from the low permeability formation would result in lower total wellbore storage during shut-in.

Fig. (**3**) shows a trend of gradual surface casing pressure buildup, but different permeability have different rates to achieve the initial pressure stabilization. That is, with smaller annular gas volume and the same reservoir pressure, low permeable formations would build-up its wellbore pressure faster than highly permeable formations.

3.2. Simulation of Gas Migration at Nominal Gas Inflow Volume

1.5 m^3 of gas is assumed to flow into the annulus, the trends of bottom hole pressure, inflow gas volume and surface casing pressure with shut-in time are shown in Figs. (**4-6**).

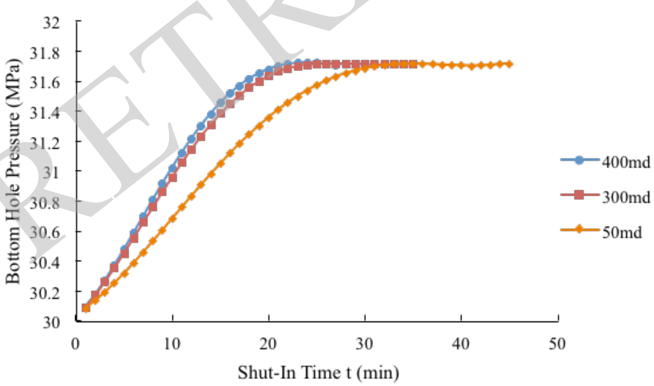

Fig. (4). Bottom hole pressure for an assumed gas kick volume at well shut-in.

Figs. (**4**, **6**) shows that wellbore and casing pressure increase with increase in shut-in time as a consequence of gas upward migration. When wellbore pressure equalizes the reservoir pressure, surface casing and bottom hole pressures stabilized. On the other hand, the rates of rise of the bottom-hole and surface casing pressures for the 50-md reservoir are slower than for the 300 or 400-md permeability formations, which are opposite to the results presented in Figs. (**1**, **3**). This is because for the same reservoir pressurization and equal initial annular gas volume at the time of complete well shut-in, the higher rate of gas inflow from the 300 or 400-md formations would continuously introduce larger quantity of gas mass into the annulus than the 50-md formation. Since the annular gas volume is the same for all the permeability cases, the introduction of larger gas mass by the 300 or 400-md formation would result in rapid increase in the annular gas density up to the maximum gas density.

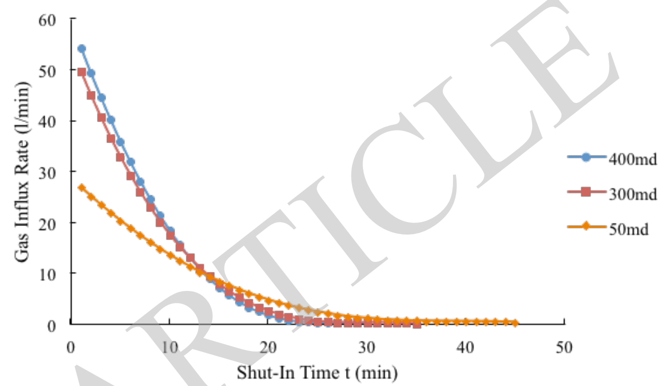

Fig. (5). Inflow gas volume for an assumed gas kick volume at well shut-in.

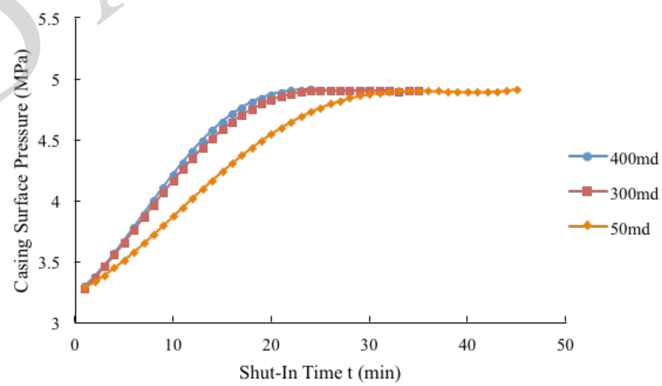

Fig. (6). Surface casing pressure for an assumed gas kick volume at well shut-in.

Such rapidity of gas density increase also causes rapid decline in the subsequent inflow rate from the 300 or 400-md formations. A shut-in time is reached when the rates of inflow from the formations are equal, as shown by the intersection point in Fig. (**5**). When the maximum annular gas density is attained, initial pressure stabilization occurs at the surface and downhole.

4. MODEL VALIDARION

In order to validate the model, the experimental results of Goldking No.1 Well at Louisiana State University (LSU) [11] is used, which is presented in Fig. (**7**).

As shown in Fig. (**7**), pressure rise slowly in the system during the first shut-in period. Such period is considered as the wellbore storage period because more gas could be injected into the closed annulus to attain the initial wellbore

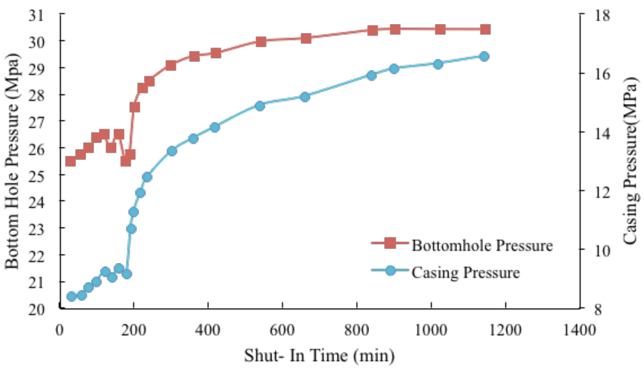

Fig. (7). Plots of the gas kick experimental results at LSU-Goldking NO.1 Well.

pressure rise during shut-in. After attaining a desired casing pressure, the gas injection was stopped, and the casing pressure was maintained by bleeding the mud from the well. During this period, the drop in the bottom-hole pressure is as a result of gas bubble expansion, which consequently lowers the equivalent hydrostatic pressure of the gas-mud mixture in the annulus with constant casing pressure. When gas bubble reaches the surface choke line, there is a sharp increase in the casing pressure, which also causes sharp increase in the bottom-hole pressure as shown the final shut-in period in Fig. (**7**). That is because the gas bubbles exert the high internal pressure on the surface choke. Comparison results show that the simulation results of the proposed model have a good agreement with the experimental results.

CONCLUSION

(1) Based on wellbore storage effect, a new model to the wellbore and casing pressure build-up during shut-in for a gas kick well is developed. And the accuracy of the model has been validated with experimental results.

(2) At different gas kick volumes, as shut-in time increases, wellbore and casing pressure increase. The rate of bottom-hole pressure rise increases as the permeability decreases. And surface casing pressure stabilizes quickly for low permeable formations.

(3) At equal initial annular gaseous volume, as shut-in time increases, wellbore and casing pressure increase. And the rates of rise of the bottom-hole and surface casing pressures for low permeable formations are slower than for high permeability formations.

CONFLICT OF INTEREST

The authors confirm that this article content has no conflict of interest.

ACKNOWLEDGEMENTS

The support of the National Natural Science Foundation of China (No. 51374077) is gratefully acknowledged.

REFERENCES

[1] Rongrong, S.; Baojiang, S.; Xiaolan, L.; Zhiyuan, W. Calculation and analysis of bottomhole pressure in wellbore after gas invasion. *Fault-Block Oil Field*, **2011**, *18*(4), 486-488.

[2] Grace, R.D. *Advanced Blowout and Well Control*. Gulf Publishing Company: Houston, Texas, **1994**.

[3] Li, X.F.; Zhuang, X.Q.; Sui, X.; Gang, T. Study on two-phase gas-liquid flow during gas kick. *J. Eng. Thermophys.*, **2004**, *25*(1), 73-76.

[4] Hasan, A.R.; and Kabir, C.S. *Modeling Changing Storage During a Shut-in Test*. SPE 24717, 67th Annual Technical Conference and Exhibition, Washington, Oct. 4-7, **1992**.

[5] Lu, Z.; Gao, X.; Cao, X. Simulation study on two-phase gas-liquid flow during gas kick. *Oil Dril. Prod. Technol.*, **2008**, *2*(30), 25-28.

[6] Terry, R.E.; Rogers, J.B.. *Applied Petroleum Reservoir Engineering*. 3rd ed.; Prentice-Hall: London, **1991**.

[7] Spiegel, M.R.; Liu, J. *Mathematical Handbook of Formulas and Tables - Schaum's Outline Series*. McGraw-Hill Companies: NewYork, **1997**.

[8] Nickens, H.V. A Dynamic Computer Model of a Kicking Well: Part I-The Theoretical Model. SPE 14183, *SPE Drilling Engineering*, *Part II-Model Predictions and Conclusions*. SPE 14184, SPE Annual Technical Conference and Exhibition, Las Vegas, Sep. 22-26, **1985**.

[9] Butler, G. *Multiphase Flow Consideration in Underbalanced Drilling of Horizontal Well,* 7th International Conference on Multiphase Production, Cannes, France, June 7-9, **1995**.

[10] Beggs, H.; Brill, J. A study of two phase flow in inclined pipes. *J. Petrol. Technol.*, **1973**, *25*(5), 607-617.

[11] Mathews, J.L.; Bourgoyne, A.T. *Well Control - How to Handle a Gas Kick Moving up a Shut-in Well*. SPE Reprint Series, No. 42, **1996**.

Received: November 26, 2014 Revised: January 28, 2015 Accepted: February 6, 2015